Parameters optimization of terahertz negative dynamic conductivity in optically and electrically pumped graphene structures

LIU YA-QING[a], REN GUANG-JUN[a*], ZHANG YU-PING[b], CAO YAN-YAN[b], ZHANG HUI-YUN[b]

[a] *School of Electronics Information Engineering; Tianjin Key Lab. Of Film Electronic & Communication Devices; Engineering Research Center of Communication Devices and Technology, Ministry of Education; Tianjin University of Technology; Tianjin 300384, PR China;*

[b]*Qingdao Key Laboratory of Terahertz Technology, College of Science, Shandong University of Science and Technology, Qingdao 266510, PR China;*

We study parameters optimization of negative dynamic conductivity in terahertz range of frequencies in optically and electrically pumped graphene structures. Graphene structures consist of single-graphene-layer (SGL) structures and multiple-structure-layer (MGL) structures. The optimization of parameters including quasi-Femi energy, effective temperature, electron-hole momentum relaxation time and the number of graphene layer (GL) etc. were studied systematically. From the simulations we find that the negative dynamic conductivity in optically pumped graphene structures can be largest when effective temperature $T = 50K$, relaxation time $\tau = 10\,ps$, quasi-Femi energy $\varepsilon_F = 55meV$ and the number of GL $K = 120$. The negative dynamic conductivity in electrically pumped graphene structures can be largest when $T = 50K$, $\tau = 10\,ps$, bias voltage $V = 120meV$ and low gate voltage. Meanwhile, the negative dynamic conductivity can be larger in electrically pumped graphene structures than that in optically pumped graphene structures.

Received August 25, 2014; accepted May 7, 2015)

Keywords: Terahertz, Graphene, Negative dynamic conductivity, Parameters optimization

1. Introdution

Graphene is a single layer of carbon atoms packed into a dense two-dimensional honeycomb crystal structure. Graphene has drawn wide attention since it was found. It has novel photoelectric properties, magnetic properties and other special properties[1]. Due to the gapless energy spectrum and the relaxation characteristics of the carriers, the real part of the dynamic conductivity can be negative corresponding to the population inversion in both optically or electrically pumped SGL structures and MGL structures in the terahertz frequency range[2-6]. Therefore, graphene can act as the active medium in a terahertz laser and can be used in photoelectric devices[7-8].

The dynamic conductivity in optically or electrically pumped SGL/MGL has been studied widely. V. Ryzhii et al. studied the dynamic conductivity in optically pumped SGL and MGL disregarding the thermo effect[2-3]. They studied the dynamic conductivity in optically pumped SGL considering the thermo effect[9]. In addition, they give the function of the dynamic conductivity of two kinds of double-graphene-layer structures[10]. A. Satou et al. studied the dynamic conductivity in optically pumped SGL as well[11]. Y. P. Zhang et al. studied the dynamic conductivity in optically and electrically pumped MGL[4,6]. M. Ryzhii et al. have studied the dynamic conductivity in electrically pumped SGL[5]. While a substantial amount of research has been performed for dynamic conductivity, the parameters optimization of negative dynamic conductivity have not reported.

In this paper, we study the parameters optimization of negative dynamic conductivity in terahertz frequencies range in optically and electrically pumped SGL/MGL structures. The optimization of parameters including quasi Femi energy, effective temperature, electron-hole momentum relaxation time and the number of graphene layer were studied systematically. From the simulations we find that the negative dynamic conductivity can be larger at lower temperature, longer relaxation time in optically and electrically pumped SGL/MGL structures. Meanwhile, the negative dynamic conductivity can be larger in electrically pumped graphene structures than that in optically pumped graphene structures.

2. The theory of opticaly pumped graphene

Fig.1 show the graphene structure under optically pumped. GL(s) are fabricated on the substrate in the structure. Meanwhile, the incident light with photon energy $\hbar\Omega$ irradiates on the GL(s) vertically.

The real part of dynamic conductivity consists of the contribution of interband transition and the contribution of intraband transition. The contribution of interband transition is negative and the contribution of intraband transition is positive[2].

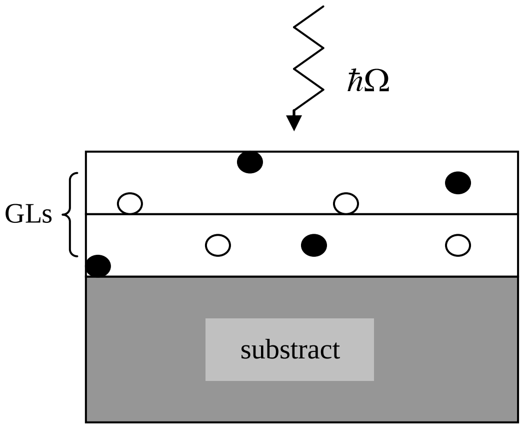

Fig.1 Schematic view of graphene structure under optically pumped

The dynamic conductivity in optically pumped SGL structures can be expressed as:

$$\mathrm{Re}\,\sigma_\omega = \mathrm{Re}\,\sigma_\omega^{inter} + \mathrm{Re}\,\sigma_\omega^{intra} = \frac{e^2}{4\hbar}\tanh\left(\frac{\hbar\omega - 2\varepsilon_F}{4k_BT}\right) + \frac{e^2}{4\hbar}\frac{8k_BT\tau}{\pi\hbar\left(1+\omega^2\tau^2\right)}\ln\left[1+\exp\left(\frac{\varepsilon_F}{k_BT}\right)\right] \quad (1)$$

where e is the electron charge, $\hbar$ is the reduced Planck constant, k_B is the Boltzman constant, T is the effective temperature, ε_F is quasi-Femi energy, and ω and τ are the frequency of emitted wave and electron-hole momentum relaxation time, respectively.

Each GL will absorb the incident radiation in optically pumped MGL, so it has a different quasi-Femi energy. The Femi energy in kth GL can be represented as[4]:

$$\varepsilon_F^{(k)} = \varepsilon_F^{(K)}\left[\left(1-\beta\right)^{K-k}\right]^{\gamma} \quad (2)$$

where $\varepsilon_F^{(K)} = \varepsilon_F^{T}$ is the quasi-Femi energy of top GL, $\beta = \pi e^2/\hbar c \approx 0.023$ is the absorption coefficience of each GL, and K and γ are the number of GLs and phenomenological parameter, respectively.

The dynamic conductivity of kth GL can be expressed as[3,12]:

$$\mathrm{Re}\,\sigma_\omega^{(k)} = \frac{e^2}{4\hbar}\tanh\left(\frac{\hbar\omega - 2\varepsilon_F^{(k)}}{4k_BT}\right) + \frac{e^2}{4\hbar}\frac{8k_BT\tau}{\pi\hbar\left(1+\omega^2\tau^2\right)}\ln\left[1+\exp\left(\frac{\varepsilon_F^{(k)}}{k_BT}\right)\right] \quad (3)$$

The dynamic conductivity of MGL is the sum of dynamic conductivity of each GL. It can be expressed as:

$$\mathrm{Re}\,\sigma_\omega = \sum_{k=1}^{K}\mathrm{Re}\,\sigma_\omega^{(k)} = \frac{e^2}{4\hbar}\sum_{k=1}^{K}\tanh\left(\frac{\hbar\omega - 2\varepsilon_F^{(k)}}{4k_BT}\right) + \frac{e^2}{4\hbar}\sum_{k=1}^{K}\frac{8k_BT\tau}{\pi\hbar\left(1+\omega^2\tau^2\right)}\ln\left[1+\exp\left(\frac{\varepsilon_F^{(k)}}{k_BT}\right)\right] \quad (4)$$

3. The theory of electricaly pumped graphene structures

Fig. 2 shows the graphene structure under electrically pumped. The structure in consideration has two split gate. The gate voltages are assumed as $V_n = V_g/2$ and

$V_p = -V_g/2$, respectively. The n region and p region can be formed when the bias voltage V is applied.

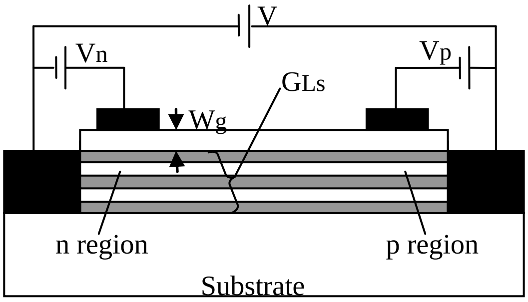

Fig.2 Schematic view of graphene structure under electrically pumed

The quasi-Femi energy can be controlled by the gate voltage, which can be represented as[5]:

$$\varepsilon_F \approx \hbar \upsilon_F \sqrt{\frac{\varepsilon V_g}{4eW_g}} \tag{5}$$

Where $\upsilon_F = 1.0\times10^8 cm/s$ is the Feimi velocity, ε is the electron (hole) energy, and V_g and W_g are the gate voltage and the thickness of the gate layer, respectively.

The dynamic conductivity in electrically pumped SGL structures can be expressed as:

$$\mathrm{Re}\,\sigma_\omega = \mathrm{Re}\,\sigma_\omega^{intra} + \mathrm{Re}\,\sigma_\omega^{inter} = \frac{e^2\varepsilon_F\tau}{2\pi\hbar^2\left(1+\omega^2\tau^2\right)} + \frac{e^2}{2\hbar}\exp\left(\frac{eV-2\varepsilon_F}{2k_BT}\right)\sinh\left(\frac{\hbar\omega-eV}{4k_BT}\right) \tag{6}$$

Each GL has different quasi Femi energy in electrically pumped MGL. The Femi energy in kth GL can be represented as:

$$\varepsilon_F^k = \frac{eV_g}{2}\psi_k \tag{7}$$

Where ψ_k can be obtained by solving Poisson equation.

The dynamic conductivity of kth GL can be expressed as [6]:

$$\mathrm{Re}\,\sigma_\omega^k = \frac{e^2}{2\hbar}\exp\left(\frac{eV-2\varepsilon_F^k}{2k_BT}\right)\sinh\left(\frac{\hbar\omega-eV}{4k_BT}\right) + \frac{e^2\varepsilon_F^k\tau}{2\pi\hbar^2\left(1+\omega^2\tau^2\right)} \tag{8}$$

The dynamic conductivity of MGL is the sum of dynamic conductivity of each GL. It can be expressed as:

$$\mathrm{Re}\,\sigma_\omega = \sum_{k=1}^{K}\mathrm{Re}\,\sigma_\omega^{(k)} = \sum_{k=1}^{K}\frac{e^2\varepsilon_F^k\tau}{2\pi\hbar^2\left(1+\omega^2\tau^2\right)} + \sum_{k=1}^{K}\frac{e^2}{2\hbar}\exp\left(\frac{eV-2\varepsilon_F^k}{2k_BT}\right)\sinh\left(\frac{\hbar\omega-eV}{4k_BT}\right) \tag{9}$$

4. Numerical simulation and analysis of results

In this study, the real part of the dynamic conductivity is normalized by $e^2/4\hbar$. It is assumed that $W_g = 10nm$.

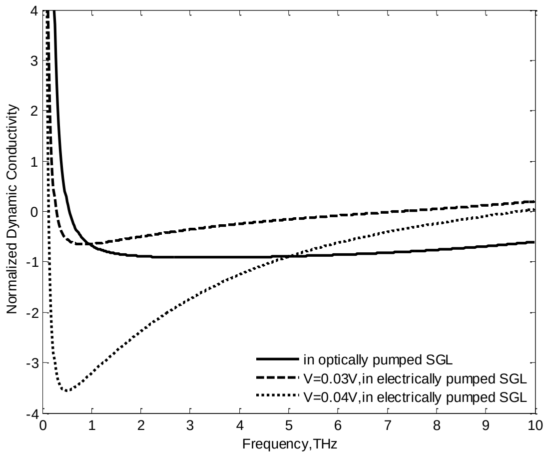

Fig.3 Frequency dependence of the normalized dynamic conductivity

Fig.3 shows the frequency dependence on the real part of the dynamic conductivity in two different cases at $T = 77K$, $\varepsilon_F = 30meV$, and $\tau = 10ps$. The first case corresponds to optically pumped SGL, while the other case corresponds to electrically pumped SGL. In the second case, we take different bias voltages $V = 30mV$ and $V = 40mV$. The dynamic conductivity can be negative in terahertz range of frequencies and the negative dynamic conductivity with small bias voltage in the second case is much smaller than that of the first case. However, the negative dynamic conductivity can be larger with higher bias voltage. It will exceed that of the first case. The concentration of the carriers increases with the increase of bias voltage, which can benefit to the production of terahertz radiation. Therefore, the negative dynamic conductivity of electrically pumped graphene with a high bias voltage is much larger than that of optically pumped graphene.

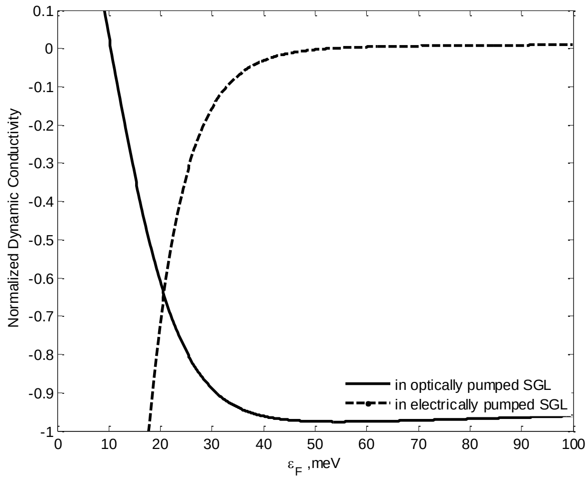

Fig.4 Quasi-Femi energy dependence of the normalized dynamic conductivity

Fig.4 shows quasi-Femi energy dependence on the dynamic conductivity in optically and electrically pumped SGL at $\omega / 2\pi = 7THz$, $T = 77K$, and $\tau = 10ps$. The solid line represents SGL under optically pumped. The dotted line represents SGL under electrically pumped, in which $V = 30meV$. The negative dynamic conductivity increases with the increase of the quasi-Femi energy in optically pumped SGL, while it decreases in electrically pumped SGL. The normalized dynamic conductivity is almost saturated at high quasi-Femi energy. The production of terahertz radiation will increase with the increase of the photon energy of incident light in optically pumped SGL. However, due to the quantum effect, it cannot increase continuously when photon energy is large enough. Therefore, it's important to choose quasi-Femi energy properly to get largest negative conductivity.

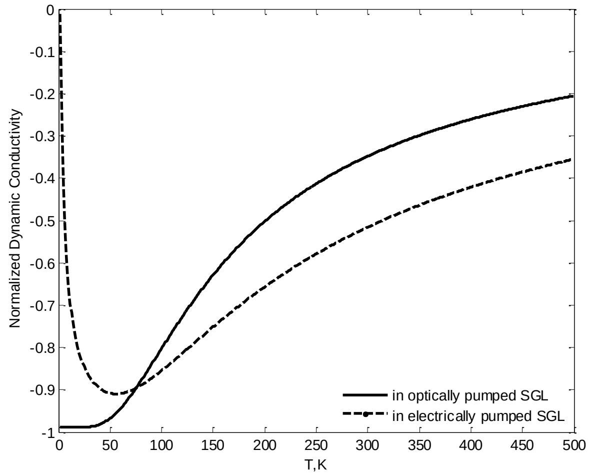

Fig.5 Effective temperature dependence of the dynamic conductivity

Fig.5 shows effective temperature dependence on the dymamic conductivity in optically and electrically pumped SGL at $\omega / 2\pi = 7THz$, $\varepsilon_F = 30meV$, and $\tau = 10ps$. The solid line represents SGL under optically pumped. The dotted line represents SGL under electrically pumped, in which $V = 30meV$. The negative dynamic conductivity can reach the maxium value at low effective temperature, and it decreases with the increase of effective temperature. The normalized dynamic conductivity can get maximal value at about $T = 50K$. The carriers are in the condensed state at low effective temperature. The interaction is strong between carriers. However, the carriers are active at high effective temperature. The damping is larger than that at lower effective temperature. Therefore, the negative conductivity have a maximum value at moderate effective temperature.

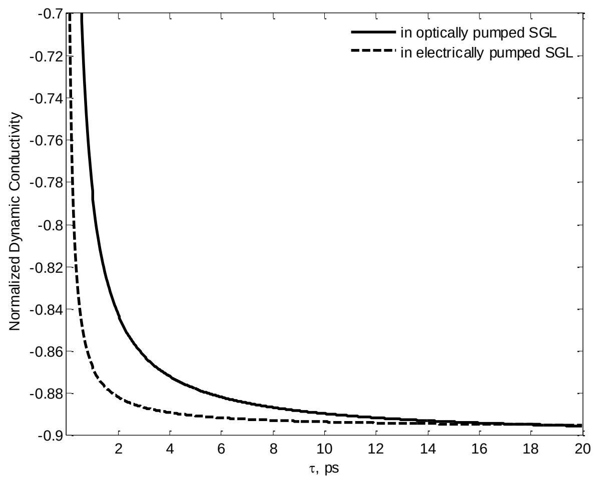

Fig.6 Electron (hole) momentum elaxation time dependence of the dynamic conductivity

Fig.6 shows electron (hole) momentum relaxation time dependence on the dynamic conductivity in optically and electrically pumped SGL at $T = 77K$, $\omega / 2\pi = 7THz$, and $\varepsilon_F = 30meV$. The solid line represents SGL under optically pumped. The dotted line represents SGL under electrically pumped, in which $V = 30meV$. The negative dynamic conductivity increases with the increase of electron (hole) momentum relaxation time, and it is almost unchanged when the electron (hole) momentum relaxation time is larger than 10ps. The longer electron (hole) momentum relaxation time, the higher doping concentration of graphene. When the electron (hole) momentum relaxation time is longer, the collision between carriers is strong and it will be in a stable state. If the electron (hole) momentum relaxation time is big enough, the quality of graphene is worse. Therefore, the large negative conductivity can be achieved by choosing graphene with momentum relaxation time $\tau = 10ps$.

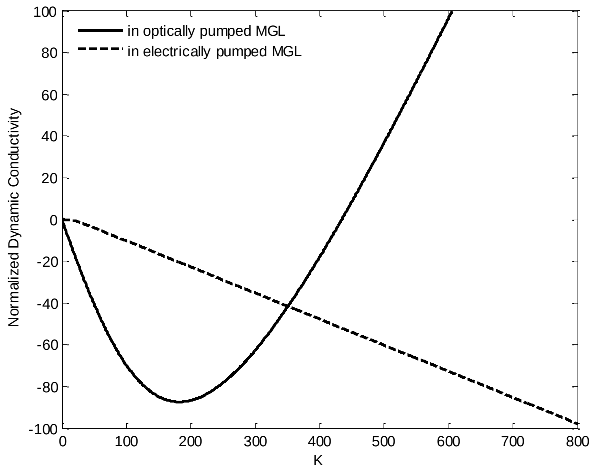

Fig.7 The number of GLs dependence of the dynamic conductivity

Fig.7 shows the number of GLs dependence on the dynamic conductivity in optically and electrically pumped MGL at $\omega / 2\pi = 7THz$, $\varepsilon_F = 30meV$, $T = 77K$, and $\tau = 10ps$. The solid line represents SGL under optically pumped. The dotted line represents SGL under electrically pumped, in which $V = 30meV$.

The negative dynamic conductivity increases first and decreases with the increase of the number of GLs in optically pumped MGL, while it keeps increasing in electrically pumped MGL. Due to each GL will absorb incident radiation, the optical radiation will attenuate in optically pumped GL. If the number of GLs is big, there will be no light to get GL at bottom. Meanwhile, the dynamic conductivity GLs which get weak optical radiation will be positive. So the negative dynamic conductivity has optimization when choosing proper number of GLs.

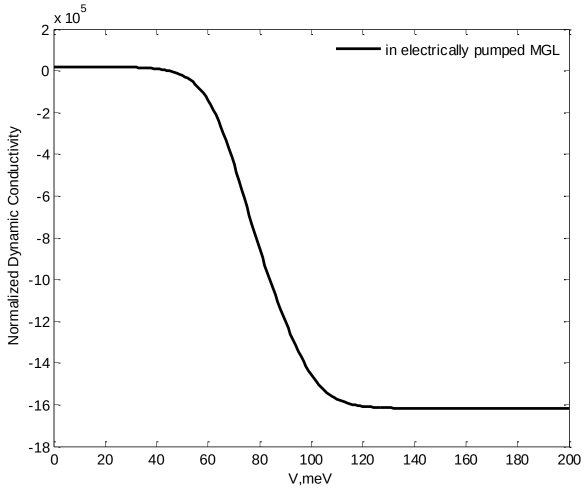

Fig.8 Bias voltage dependence of the dynamic conductivity

Fig.8 shows bias voltage dependence on the dynamic conductiviy in electrically pumped MGL at $K = 3$, $\omega / 2\pi = 7THz$, $T = 77K$, $\varepsilon_F = 30meV$ and $\tau = 10ps$. The solid line represents SGL under optically pumped. The dotted line represents SGL under electrically pumped, in which $V = 30meV$. The negative dynamic conductivity increases first and then keeps constant with the increase of bias voltage. It can get maximal value at about $V = 100meV$. The concentration of induced carriers increases with the increase of bias voltage. When the bias voltage is high enough, the carriers is in the saturation state. Hence, the largest negative conductivity can be got with low temperature at about $V = 100meV$.

5. Conclusion

In summary, according to the theory of optically and electrically pumped SGL/MGL structures, we study the parameters optimization of negative dynamic conductivity in terahertz range of frequencies. The optimization of parameters include quasi Femi energy, effective temperature, electron-hole momentum relaxation time and the number of graphene layer. The negative dynamic conductivity can be larger in electrically pumped graphene structures than that in optically pumped graphene structures. In addition, the negative conductivity in optically pumped graphene structures can be largest when effective temperature $T = 50K$, relaxation time $\tau = 10\,ps$, quasi-Femi energy $\varepsilon_F = 55meV$ and the number of GL $K = 120$. The negative dynamic conductivity in electrically pumped graphene structures can be largest when $T = 50K$, $\tau = 10\,ps$, bias voltage $V = 120meV$ and low gate voltage.

Acknowledgments

This work was supported by the National Natural Science Foundation of China (Grant No. 61001018), the Natural Science Foundation of Shandong Province, China (Grant No. ZR2011FM009, ZR2012FM011), the Research Fund of Shandong University of Science and Technology (SDUST), China (Grant No. 2010KYJQ103), the SDUST Research Fund (Grant No. 2012KYTD103), the Shandong Province Higher Educational Science and Technology Program project (Grant No.J11LG20), the Qingdao Science & Technology Project (Grant No.11-2-4-4-(8)-jch), and the Qingdao Economic & Technical Development Zone Science & Technology Project (Grant No.2013-1-64).

References

[1] K. S. Novoselov, A. K. Geim, S. V. Morozov, D. Jiang, M. I. Katsnelson, I. V. Grigorieva, S. V. Dubonos, A. A. Firsov, Nature **438** 197 (2005)
[2] V. Ryzhii, M. Ryzhii, and T. Otsuji, J. Appl. Phys. **101** 083114 (2007)
[3] V. Ryzhii, M. Ryzhii, A. Satou, T. Otsuji, A. A. Dubinov, and V. Ya. Aleshkin, J. Appl. Phys. **106,** 084507 (2009)
[4] Y. P. Zhang, L. Y. Liu, X. Zhang, H. Y. Zhang, H. Y. Zhang, Journal of Optoelectrics • Laser, **23,** 5 (2012)
[5] M. Ryzhii, V. Ryzhii, JPN. J. Appl. Phys. **46** 151 (2007)
[6] Y. P. Zhang, H. Y. Zhang, Y. H. Yin, L. Y. Liu, X. Zhang, Y. Gao, and H. Y. Zhang, Acta Phys. Sin. **61** 047803 (2012)
[7] T. Otsuji, S. B. Tombet, A. Satou, M. Ryzhii, V. Ryzhii, IEEE J. Selected Topic in Quantum Electron **19** 8400209 (2013)
[8] V. Ryzhii, M. Ryzhii, V. Mitin, and T. Otsuji, J. Appl. Phys. **110,** 094503 (2011)
[9] V. Ryzhii, M. Ryzhii, V. Mitin, A. Satou, T. Otsuji, Jpn. J. Appl. Phys. **50** 094001 (2011)
[10] V. Ryzhii, A. A. Dubinov, T. Otsuji, V. Ya. Aleshkin, M. Ryzhii, and M. Shur, Optics Express **21,** 31567 (2013)
[11] A. Satou, V. Ryzhii, Y. Kurita, T. Otsuji, J. Appl. Phys. **113** 143108 (2013)
[12] A. A. Dubinov, V. Ya. Aleshkin, V. Mitin, T. Otsuji, V. Ryzhii, J. Phys.: Condens. Matter **23,** 145302 (2011)

*Corresponding author: rgj1@163.com